Computational studies of a cut-wire pair and combined metamaterials

Adv. Nat. Sci.: Nanosci. Nanotechnol. **2** (2011) 033001 (9pp) doi:10.1088/2043-6262/2/3/033001

REVIEW

Computational studies of a cut-wire pair and combined metamaterials

Thanh Tung Nguyen[1], Peter Lievens[1], Young Pak Lee[2] and Dinh Lam Vu[3]

[1] Laboratory of Solid State Physics and Magnetism, Department of Physics and Astronomy, Katholieke Universiteit Leuven, Leuven B-3001, Belgium
[2] Quantum Photonic Science Research Center and Department of Physics, Hanyang University, Seoul 133–791, Korea
[3] Institute of Materials Science, Vietnam Academy of Science and Technology, 18 Hoang Quoc Viet, Hanoi, Vietnam

E-mail: lamvd@ims.vast.ac.vn, peter.lievens@fys.kuleuven.be and yplee@hanyang.ac.kr

Received 13 April 2011
Accepted for publication 7 June 2011
Published 1 July 2011
Online at stacks.iop.org/ANSN/2/033001

Abstract
The transfer-matrix method and finite-integration simulations show how the transmission properties of combined metamaterials, which consist of metallic cut-wire pairs and continuous wires, are affected by geometric parameters. The corresponding effective permittivity and permeability are retrieved from the complex scattering parameters using the standard retrieval procedure. The electromagnetic properties of the cut-wire pair as well as the left-handed behavior of the combined structure are understood by the effective medium theory. In addition, the dimensional dependence of transmission properties, the shapes of cut-wire pairs and continuous wire, and the impact of dielectric spacer are both examined. Finally, by expanding the results of previous research (Koschny *et al* 2003 *Phys. Rev. Lett.* **93** 016608), we generalize the transmission picture of combined structures in terms of the correlation between electric and magnetic responses.

Keywords: metamaterials, left-handed materials, cut-wire pair, electromagnetic

Classification number: 5.17

1. Introduction

The terminology 'left-handed materials (LHMs)' to classify materials, which exhibit a negative index of refraction with simultaneously negative permittivity and permeability, was proposed more than four decades ago by Veselago [1]. Afterwards, the first practical realization of LHM was shown in Smith's experiments [2], based on Pendry's suggestion [3, 4]. There, the negative refractive index is composed of a periodic array of split-ring resonators (SRRs), providing a magnetically negative permeability and continuous wires with a negative permittivity below the plasma frequency. This combination has been used widely to study and fabricate LHMs [5–7]. Recently, a progressive design called cut-wire pair (CWP), which is a continued transformation of the symmetric SRR, has received considerable interest due to its advanced properties [8, 9], especially for optical implementations [10, 11]. The combined structure of CWPs and continuous wires are now recognized as an advanced structure for left-handed (LH) behavior at high frequencies. Their great potential has been confirmed in recent research where the negative refraction is presented in a three-dimensional optical metamaterial [12].

There is a series of computational work [13–16] where the important transmission and reflection properties of CWP/SRR-based LHMs have been investigated for both microwave and optical frequencies. It was proven that characteristic understanding as well as parameter optimization are important issues in studying LHMs. Moreover, it has been revealed that the combination of CWPs/SRRs with continuous wires does not always guarantee the LH behavior. In fact, the electric response of the combined structure results

from both continuous wires and CWPs/SRRs rather than from only continuous wires, since the CWPs/SRRs also exhibit the electric resonance in addition to the original magnetic one [8, 17]. The electric response of CWPs was clarified by closing the air gap to eliminate the magnetic response. Then the electromagnetic behavior of closed CWPs is identical to that of CWs. This also explains why the plasma frequency of combined structures is always lower than that of the continuous wires only [18]. This important consideration, called the effective medium theory, has been widely applied in experimental realizations of LH behavior [11, 19].

In this paper, we report on a comprehensive study of the electric and the magnetic properties of CWP and CWP-based combined metamaterials. The transmission and the reflection of CWPs and combined structures are calculated by utilizing the transfer matrix method [20] and the finite-integration simulation [21]. The effective parameters are also extracted from transmission, reflection and phase by performing the standard retrieved method proposed by Chen *et al* [22]. The advantage is that the correct branch of effective refractive index is correctly determined without classical ambiguity. The electromagnetic behavior of an LH medium, hence, is quantitatively characterized by the retrieval effective parameters.

This paper is organized as follows. In section 2, we discuss the characteristics of CWP structures and how the geometric parameters affect the electric and magnetic responses. The LH behavior of the combined structure, CWPs and continuous wires, is realized by employing the effective medium theory and the retrieval method in section 3. Interestingly, in section 4, the negativity of refractive index is obtained not only when both permittivity and permeability are negative but also when only permittivity is negative. The impact of the dielectric spacer on the LH transmission as well as the dependence on the sizes of the combined structure are investigated in sections 5 and 6, respectively. Finally, we discuss the key role of the correlation between electric and magnetic components in constructing a better LH behavior or in making it disappear.

2. Characteristics of CWP structure

2.1. Electric and magnetic resonances of CWP structure

Figure 1 presents a CWP structure prepared by the continuous transformation of a two-gap symmetric SRR. As can be seen, the design of the CWP, besides its simplicity, has distinct advantages over conventional SRRs. The incident wave is normal to the plane of the CWP structure, which enables us to construct an LHM by only one layer of sample with strong responses [23]. So far, there is a common understanding that the SRR structure exhibits not only the magnetic resonance frequency (f_m) but also the electric one (f_e). So does the CWP structure. The magnetic resonance of CWPs comes from the circular currents driven by the capacitance between cut wires while the electric resonance is a result of the symmetric mode with parallel currents [8].

Here we discuss the electromagnetic response of the CWP structure differently from three well-known methods. To begin, we apply the effective medium analysis, which

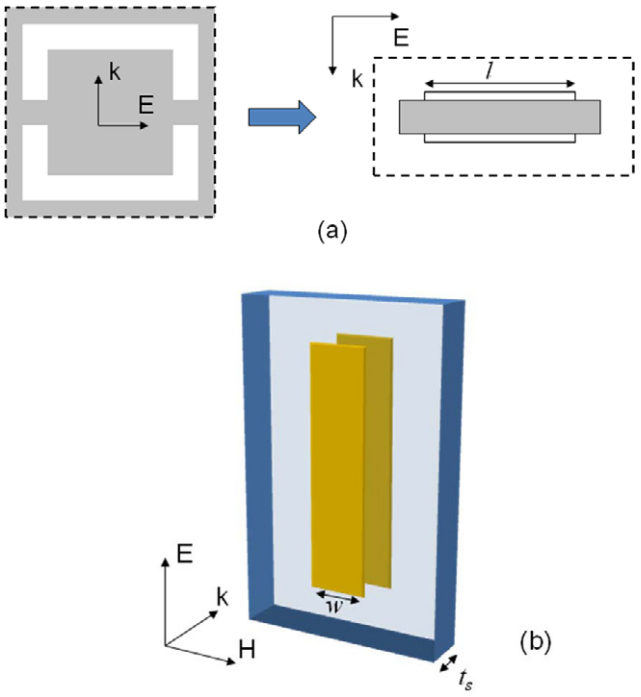

Figure 1. (a) A two-gap symmetric SRR can be transformed into a pair of parallel metallic cut wires separated by a dielectric spacer. (b) A CWP structure consists of two metallic cut wires located on both sides of a dielectric board. The width and the length of the cut wire are w and l, respectively. The thickness of the dielectric spacer is denoted by t_s.

is presented in figure 2(a). Evidently, one can observe two resonant bands of the CWP: the first around 13.8 GHz and the second around 30 GHz. To determine whether they are electrically or magnetically originated, we close at the ends of CWP to eliminate the effective capacitance, and thus the driven force in the circular currents is removed. As expected, the first resonance disappears in the transmission spectrum of the shorted-CWP structure. This clearly indicates that the 13.8 GHz resonance is magnetically originated and the other around 30.0 GHz is the electric resonance.

We independently examine the aforementioned argument by performing the standard retrieval procedure. The effective permeability of CWP and shorted-CWP structures was calculated and presented in figure 2(b). In the case of the CWP structure, a negative permeability band is shown at 13.8 GHz, which confirms that the associated resonance is the response to the external magnetic field while the negative-permeability regime is totally removed for the shorted-CWP structure.

Considering the electromagnetic behavior with respect to the orientation and the incident field, we are also able to identify the electric and magnetic resonances of the CWP structure. Note that the magnetic resonance is actually generated by circular currents generated by an in-plane external magnetic field. Hence, the magnetic resonance should be destroyed by a normal-to-plane magnetic field. For this purpose, we study different relative orientations, i.e. the **H** field or **k** normal to the CWP plane by keeping **E** along the CWP. The transmission spectra of these configurations are presented in figure 2(c). As discussed, there are two resonance dips at 13.8 and 30.0 GHz, corresponding to the magnetic and electric responses, respectively, in case **k** is normal to

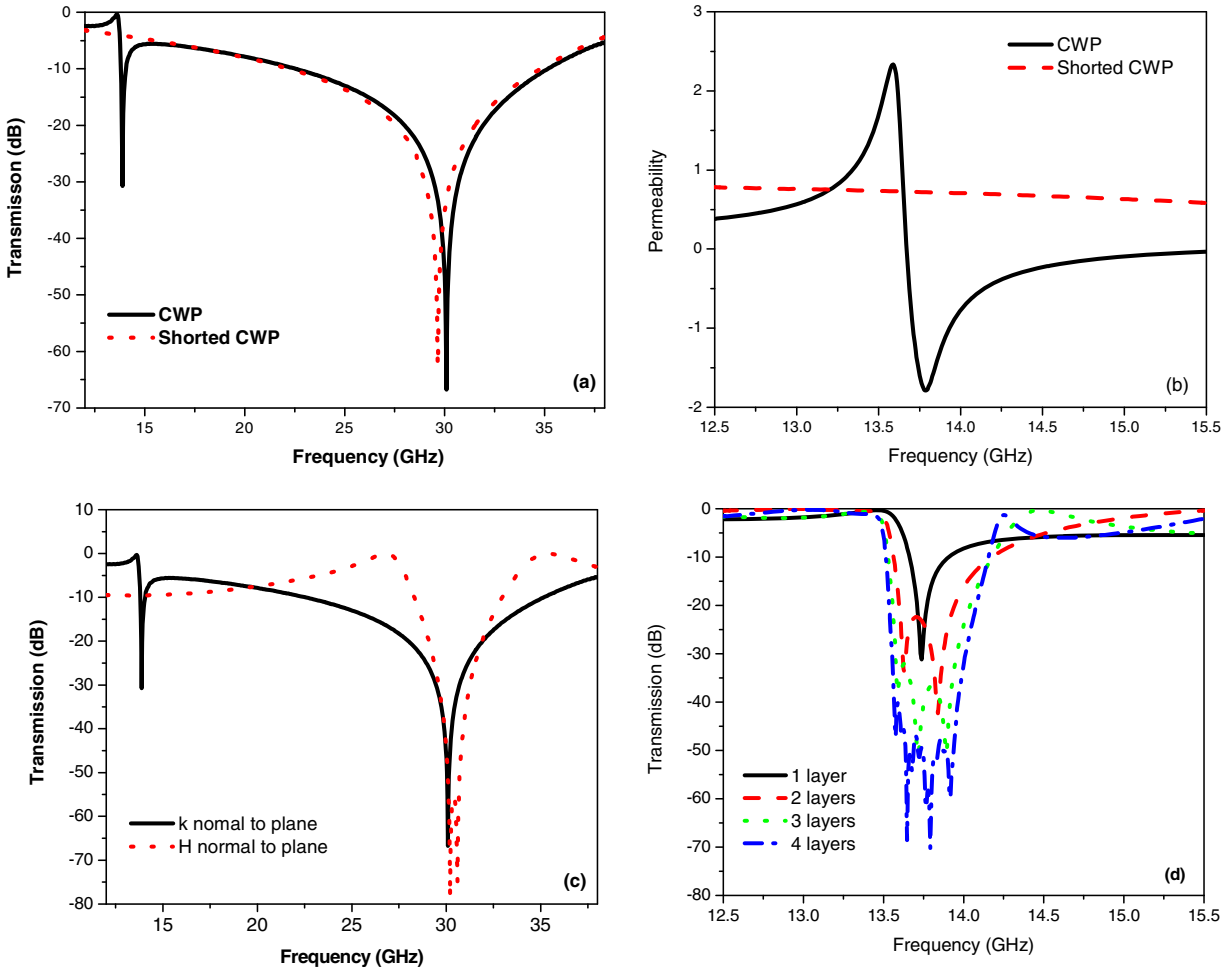

Figure 2. (a) Transmission and (b) permeability spectra of CWP and shorted CWP structures according to frequency. (c) Transmission spectra of the CWP structure for two relative orientations of incident electromagnetic waves. Only one layer along the **k**-direction is considered in (a), (b) and (c). (d) Transmission spectra of the CWP structure according to layer number. The length and width of the cut wire are 5.5 and 1.0 mm, respectively. The CWP is assumed to be made of copper with a conductivity of 5.9×10^7 S^{-1}. The thickness of the dielectric spacer is 0.4 mm. The CWP is embedded in air with periodicities of 2.0, 7.5 and 3.5 mm along the **k**, the **E** and the **H** directions, respectively.

the CWP plane. However, the magnetic resonance disappears when **H** is normal to the plane of the CWP. The reason is that for **H** normal to the CWP plane, there is no magnetically induced circular current between the two CWs, and hence no magnetic resonance is observed. The second resonance, which is the electric response, is nearly unchanged in both cases.

In figure 2(d), we present the difference in the transmission spectra of the CWP structure according to the number of layers. The periodicity along the **k**-direction is fixed at 2.0 mm. Clearly, the magnetic resonance band is strengthened and broadened by increasing the layer number.

2.2. Width and length of cut wire in tuning the electromagnetic resonances

The role of the total electric plasma frequency, f_p, in forming the LH behavior has been studied elsewhere [24], in which f_p can be taken as the sum of the electric responses from CWPs and continuous wires. It was found that the LH behavior is best achieved only if f_m is lower than f_p. Without change in the continuous wires, the tuning of f_m and f_e, therefore, is meaningful in controlling the LH behavior of the combined structure. In another study, it was shown that a simple equivalent LC circuit can be used to express partly the electromagnetic behavior of the CWP design [8]. To further explore this issue, we examine the dependence of f_m and f_e on the relative sizes of the cut wires, as shown in figure 3. The CWP medium is assumed to be constructed by the periodic arrays of CWP unit cells in figure 1(b). The corresponding lattice constants along **H**, **E** and **k** are $a_x = 3.5$, $a_y = 7.5$ and $a_z = 3.0$ mm, respectively. Only the case of **k** normal to the plane is considered. f_m and f_e are plotted as a function of a_x/w in figure 3(a) and a_y/l in figure 3(b). It can be seen that, with increasing width of the cut-wire, both f_m and f_e change, however, in different ways. While f_m shifts slightly to higher frequencies, f_e is drastically shifted downward. When f_e is close to f_m by a certain value, f_p can be lower than f_m. At that time, the LH properties are destroyed. This point is discussed in more detail in section 3. Note that the dependence of f_e on a_x/w is more significant than f_m. Therefore, one might think that the relative factor of a_x/w is useful for handling f_e; in other words, f_p with minor effect on f_m.

Figure 3(b) shows the linear dependences of f_m and f_e on a_y/l, which well supports the *LC* model proposed by Zhou *et al* [8]. Both f_m and f_e seem to be sensitive to the length l of the CWP. Importantly, a shorter l provides a significantly

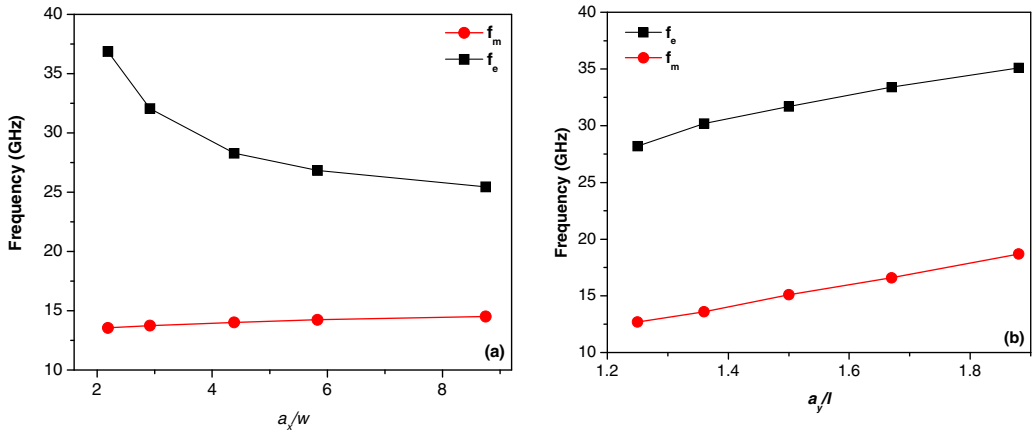

Figure 3. (a) f_{m} and f_{e} according to a_x/w, where a_x is the lattice constant in the **H**-direction, and w is the width of CWs. (b) f_{m} and f_{e} according to a_y/l, where a_y is the lattice constant in the **E**-direction and l is the length of the CWs. **k** is perpendicular to the structure plane. Only one layer along the **k**-direction is considered. Other parameters are defined in figure 2.

higher f_{m}, which is the key in pushing the LH behavior to the optical range.

3. LH behavior of a combined structure

We have already discussed several geometric parameters, which show important effects on f_{m} and f_{e} of the CWP structure. By adding continuous wires, the magnetically negative permeability is combined with a negative permittivity, and results in the LH behavior of the combined structure [25]. However, both theoretical and experimental studies of combined structures, or even possible future structures, need clear guidance in adjusting the design and optimizing the parameters. Thus, the aim of this study is to provide a systematic understanding of the parametric properties of the LH behavior in a combined structure (see figure 4).

Here, we demonstrate the nature of double-negative permittivity and permeability, as well as the negative refractive index in combined structures. In detail, we independently consider the magnetic and electric responses of combined structures using the effective medium analysis, to understand whether the LH transmission can be determined by doubly negative permittivity and permeability or not. Furthermore, the standard retrieval procedure is applied to calculate the refractive index, which should be negative for the LH behavior.

As mentioned previously, under an incident electromagnetic wave, the CWP structure exhibits a magnetic resonance, which turns out a negative permeability band. On the other hand, a periodic array of continuous wires is known to produce a wide range of negative permittivity below the plasma frequency. Thus by combining CWPs and continuous wires in a structure, one can observe the LH behavior, which is supposed to be achieved by simultaneously negative permittivity and permeability. Figure 5(a) presents a comparison of calculated transmission spectra for CWPs only, continuous wires only and a combined structure with $g = w = 1.0\,\mathrm{mm}$, $l = 5.5\,\mathrm{mm}$, $d = 4.0\,\mathrm{mm}$, $t_{\mathrm{c}} = 0.036\,\mathrm{mm}$ and $t_{\mathrm{s}} = 0.4\,\mathrm{mm}$. The structures are embedded in air with periodicities of 3.0, 7.5 and 6.0 mm along the **k**, **E** and **H**

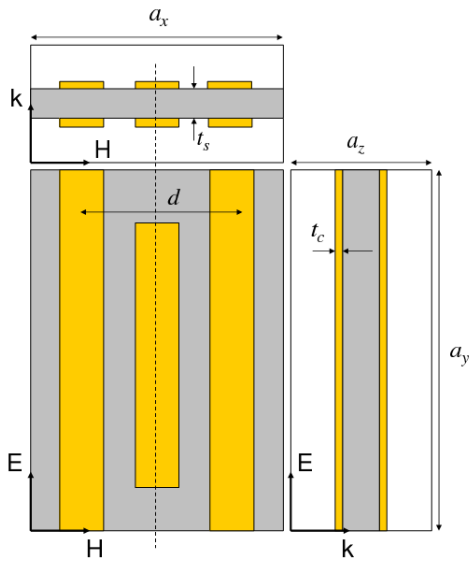

Figure 4. Geometry of the unit cell of the combined structure is viewed from the *E–H*, *E–k* and *k–H* planes. a_x, a_y and a_z are the sizes of unit cell in the *x*-, *y*- and *z*-axis, respectively. The distance between the centers of continuous wires is denoted to be d while the widths of the continuous wires and CWPs are g and w, respectively. t_{s} is the thickness of dielectric layer and that of the metal pattern is t_{c}.

directions, respectively. As can be seen, the continuous-wire structure is completely opaque from 12 to 18 GHz. This shows that the continuous wires exhibit a plasma behavior (negative permittivity) under the cut-off frequency, which is somewhat higher than the 18 GHz. The CWP structure displays a stop band around 13.8 GHz corresponding to the magnetic resonance frequency where the permeability is negative. Meanwhile, the combined structure exhibits a pass band, which exactly coincides with the stop band of the CWP structure. This means that both permittivity and permeability in this pass band of the combined structure are negative. Based on these results, it is confirmed that the pass band around 13.8 GHz in the transmission spectrum of the combined structure is clear evidence of the appearance of the LH behavior.

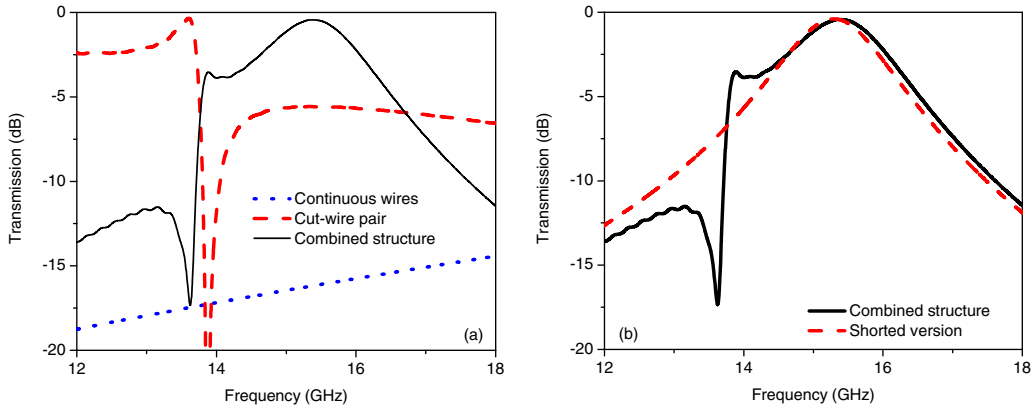

Figure 5. (a) Transmission spectra of CWPs, continuous wires and combined structures. (b) Those of the combined structure and its shorted version.

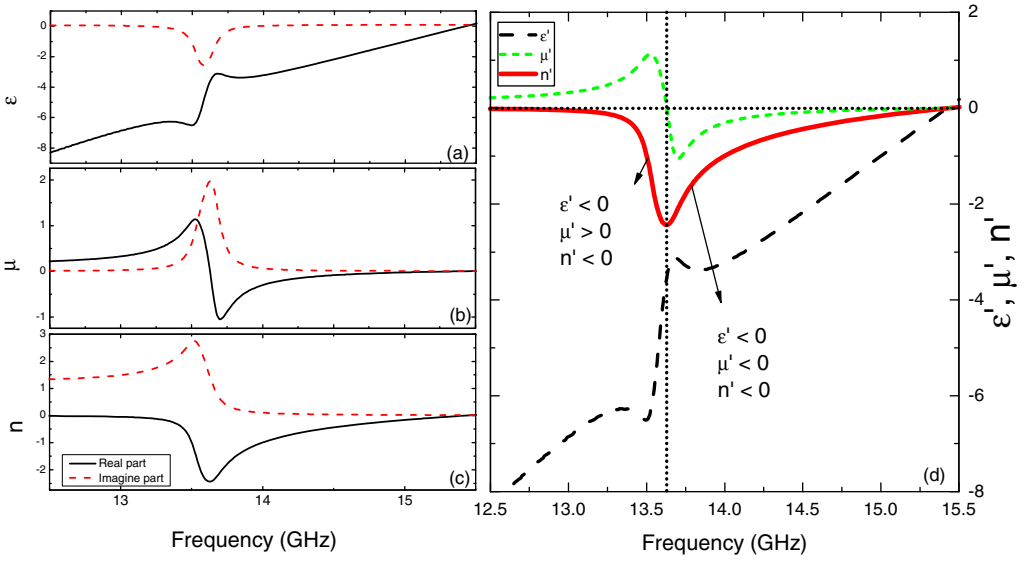

Figure 6. Calculated values of (a) ε, (b) μ and (c) n of the combined structure, defined in section 3. (d) Real parts of ε, μ and n.

In this part, we examine whether the pass band around 13.8 GHz in the combined structure results from the LH behavior or not. For this purpose, the effective medium analysis is used. The shorted combined structure, in which the CWPs are connected through the dielectric spacer at the ends of each CW, behaves as a combination of continuous and discontinuous wires. The structure is composed of a metallic pattern placed on a dielectric substrate. Both of them are nonmagnetic. Hence, it is expected that there is no magnetically negative permeability for the shorted structure, exhibiting a totally plasmonic behavior instead of the LH one. In figure 5(b), the transmission spectra for one layer of the combined structure and its shorted version are plotted. Clearly, the pass band around 13.8 GHz of the combined structure disappears in the case of the shorted version. These data imply the existence of an LH pass band based on doubly negative permittivity and permeability around 13.8 GHz. In addition, from the transmission spectrum of the shorted combined structure, the total plasma frequency of the combined structure can be qualitatively determined around 15 GHz. The second pass band at 15.5 GHz is, hence, due to right-handed behavior and still remains in the shorted version.

4. Single- and double-negative refractive index in the combined structure

Another important issue we should discuss here is the single negative refractive index of the combined structure. For this purpose, the results reported in [9] are reiterated. The complex effective μ and ε were extracted from the scattering parameters (see figures 6(a) and (b)). As shown in figure 6(d), μ and ε are simultaneously negative for frequencies higher than 13.6 GHz. Interestingly, considering the real parts only, we obtain a region of double-negative n by combining the negative μ and ε at once. However, it can be seen that the negative n region is significantly wider than the bandwidth of negative μ. For frequencies less than 13.6 GHz, μ is positive while ε is negative, but, strangely enough, n is still negative, in other words, a single-negative n. This is a peculiar feature of combined metamaterial structures, which was not completely understood previously [26–28].

Actually, in metamaterials it is possible to achieve a negative n without having simultaneously negative μ and ε if we consider both real and imaginary parts of the effective parameters. By representing the complex refractive index $n = n' + in''$, in terms of complex permittivity $\varepsilon = \varepsilon' + i\varepsilon''$ and

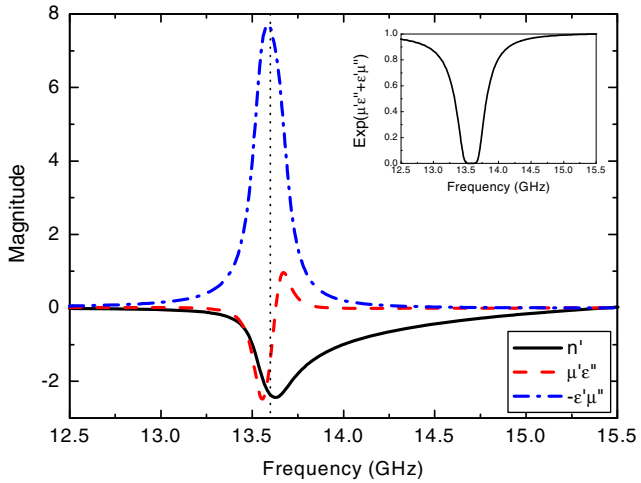

Figure 7. Retrieved values of n', $\mu'\varepsilon''$ and $-\varepsilon'\mu''$. The inset shows the calculated value of $\exp(\mu'\varepsilon''+\varepsilon'\mu'')$.

permeability$\mu = \mu' + \mathrm{i}\mu''$, we have

$$n = \sqrt{\mu\varepsilon} = \sqrt{(\mu' + \mathrm{i}\mu'') + (\varepsilon' + \mathrm{i}\varepsilon'')}, \tag{1}$$

$$= \mathrm{e}^{\mathrm{i}\phi/2}\sqrt[4]{(\mu'\varepsilon' - \varepsilon''\mu'') + (\mu'\varepsilon' + \varepsilon''\mu'')}, \tag{2}$$

where

$$\phi = \cos^{-1}\left[\frac{\mu'\varepsilon' - \mu''\varepsilon''}{\sqrt{(\mu'\varepsilon' - \mu''\varepsilon'')^2 + (\mu'\varepsilon' - \mu''\varepsilon'')^2}}\right].$$

To achieve a negative n, $\cos(\phi/2)$ needs to be negative, in other words $\mu'\varepsilon'' + \mu''\varepsilon' < 0$ [29–31]. Therefore, if the condition of $\mu'\varepsilon'' < -\mu''\varepsilon'$ is met, n can be negative without requiring both ε' and μ' to be negative and it is correct in our case. For a combined structure, the negative n can be realized in two regions as follows: single-negative and double-negative regions, as shown in figure 6(d). In the double-negative region, $\varepsilon' < 0$ and $\mu' < 0$, while $\varepsilon'' < 0$ and $\mu'' < 0$. Nevertheless, the absolute value of ε' is much larger than that of ε'' in our case, and hence it naturally provides $n < 0$. In the single-negative region below 13.6 GHz, $\varepsilon' < 0$ and while still $\varepsilon'' < 0$ and $\mu'' > 0$. In this case, simply $n < 0$ because $\mu'\varepsilon'' < -\mu''\varepsilon'$. Calculations of $\exp(\mu'\varepsilon'' + \mu''\varepsilon')$ versus frequencies show that the condition of $\mu'\varepsilon'' + \mu''\varepsilon' < 0$ is always satisfied in a range of 12.5–15.5 GHz (see figure 7). However, in the single-negative region, even though a negative n can be achieved, the high values of ε and μ'' lead to a considerable loss, in which the negative–refractive behavior is not applicable.

5. Influence of dielectric-spacer thickness

The negative permeability in the combined structure results from the circular current between paired CWs. In order to see how the coupling between paired CWs affects the LH behavior, we studied the evolution of transmission and effective parameters according to the thickness of the dielectric spacer [32]. Figure 8 presents the magnetic and electric responses of combined structures according to t_s. For this study, t_s is varied from 0.2 to 1.0 mm while the other parameters are similar to those in section 3. It can be seen that, with increasing t_s, the magnetic resonance of the combined structure slightly shifts to a higher frequency. Moreover, the negative-permeability range becomes wider as t_s is increased (figure 8(a)). Using the equivalent resonant *LC* circuit of the CWP structure [33], it is understood that the increased spacer thickness results in a decreased mutual capacitance, which in turn gives rise to a higher resonance frequency. This conclusion can also be predicted analytically in a cavity model for the coupled metallic elements [34].

Interestingly, t_s affects not only the magnetic response but also the electric one. Figure 8(b) shows that the plasma frequency f_p is noticeably shifted downward with thicker t_s. It is known that the plasma frequency of the combined structure is considered as a sum of the electric response of continuous wires and that of CWPs. The larger spacing leads to a weaker coupling between paired CWs, and thus the electric resonance of CWPs as well as f_p moves down to a lower frequency. This can be well explained by the electromagnetic analogue of molecular orbital theory through a plasmon hybridization scheme [35]. As mentioned before, the relative position between magnetic resonance and plasma frequency play a key role in constructing the LH behavior. No LH transmission is observed unless f_p is higher than the magnetic-resonant band.

We further examine this argument by calculating the transmission and refractive index of the combined structure according to t_s. Figures 9(a) and (b) indicate the evolution of transmission and refractive index by changing t_s. As expected, the negative n does not exist in the case of t_p being lower than the magnetic-resonant band (with 0.8 mm). In addition, a dip in the transmission of the combined structure at the position of the magnetic resonance is due to the single-negative permeability. As discussed above, we also observe another higher-frequency bandgap in the transmission broadened to the lower side, which corresponds to the electric resonance of CWPs.

6. Influence of periodicities

The importance of lattice constants in the magnetic and the electric resonances of the CWP structure has been reported elsewhere [36]. In this section, we investigate the influence of periodicities on the LH behavior of the combined structure. For our study, the unit cell sizes are varied from 6.0 to 7.0 mm and from 6.0 to 7.5 mm in the **H**- and the **E**-direction, respectively. The other parameters are taken from section 3. The corresponding transmission spectra of the combined structure are presented in figure 10. In figure 10(a), it can be seen that the LH behavior of the combined structure is insensitive to a_x. The LH transmission at 13.8 GHz and the right-handed band around 15.5 GHz are nearly unchanged with varying a_x. However, tuning a_y affects significantly the electromagnetic response of the combined structure. With narrower a_y, the right-handed band strongly shifts to the LH one, and entirely overlaps at $a_y = 6.3$ mm (figure 10(b)). In case of a_y smaller than 6.3 mm, the LH transmission is replaced by a dip, which is covered by the right-handed band. This is similar to the case of increasing t_s. A detailed study was presented in [37–39]. At a certain small value of

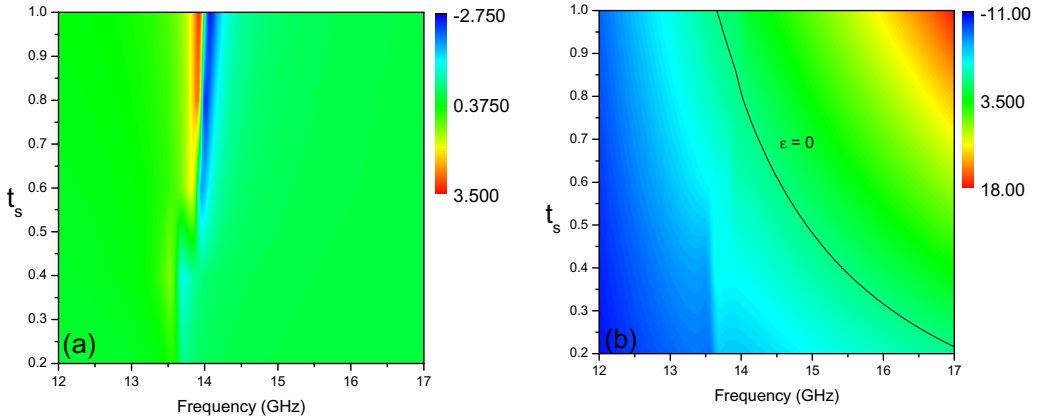

Figure 8. (a) Permeability and (b) permittivity of the combined structure according to t_s.

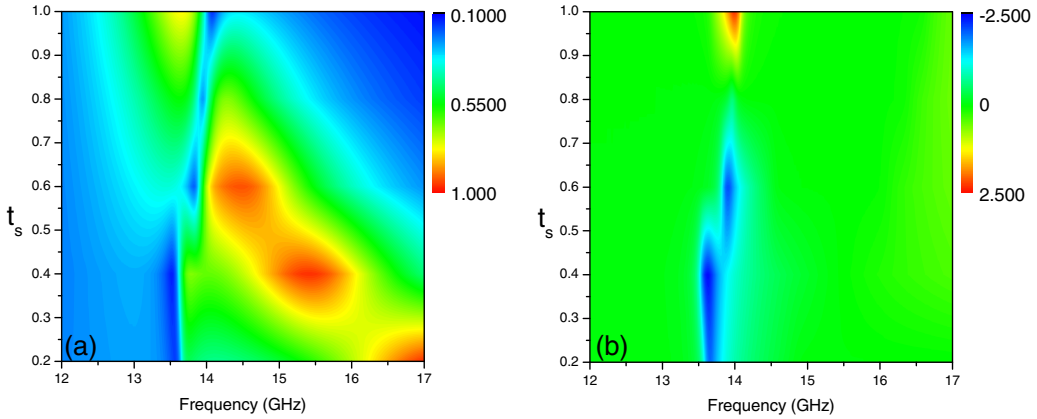

Figure 9. (a) Transmission and (b) refractive index of the combined structure according to t_s.

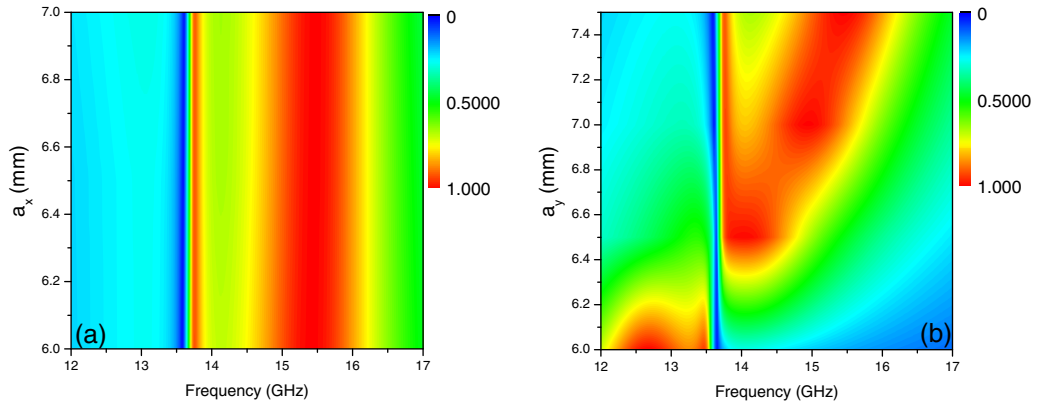

Figure 10. Transmission spectra of the combined structure according to (a) a_x and (b) a_y.

a_y, the electric resonance is very sensitive to the distance between adjacent CWs in the **E**-direction [8]. The extracted permittivity and permeability (not shown here) also confirm this explanation.

7. Electric–magnetic correlation in the combined structure

The correlation between plasma frequency and magnetic resonance band (from f_m to $f_{m'}$) in constructing the LH transmission of combined metamaterials is schematically presented in figure 11. By considering the influences of geometrical parameters on the electromagnetic response of the combined structure, one can generalize the transmission properties in terms of three possibilities. Initially, the LH behavior was analytically predicted by the effective medium theory [18] for the case of $f_m < f_{m'} < f_p$ (see the first in figure 11). However, as we realize in this study, changing t_s or a_y might bring about two other possibilities, where $f_m < f_p < f_{m'}$ and $f_p < f_m < f_{m'}$. Evidently, for the existence of LH behavior, $f_m < f_{m'} < f_p$ is not always required. It is shown that the LH transmission is still observable even with $f_m < f_p < f_m$ (the second in figure 11). For this case, the negative-permeability band is considered in two parts: the

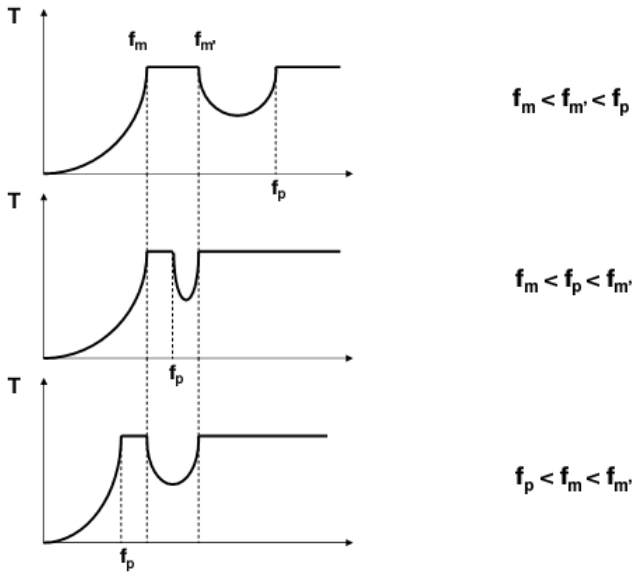

Figure 11. Transmission spectra of the combined structure according to the electric-magnetic correlation.

doubly negative permeability and permittivity from the low edge of magnetic resonance to the plasma frequency is supposed to be the LH behavior, while the remaining part with only negative permeability is not. This possibility provides a narrow LH transmission that might not be useful for the applications. This scheme also gives us an explanation for a pass band close to the magnetic resonance in the case of $f_p < f_m < f_{m'}$. Since the f_p is entirely lower than the magnetic-resonant band, the permittivity and permeability cannot simultaneously be negative. One can see a dip at the magnetic resonance and a pass band on its left side, which is due to the double-positive behavior.

8. Conclusions

Computational results were systematically presented to characterize the electromagnetic behavior of CWP and combined metamaterial structures. The electric and magnetic properties of the CWP structure were studied, based on the effective medium theory, the retrieval procedure and the response to the relative orientation of the incident wave. The strong dependence of magnetic and electric resonances of CWPs on their geometric parameters, i.e. the width and the length, were investigated. Importantly, the characteristics of LH behavior of the CWP-based combined structure were studied in detail. The impact of the dielectric spacer on the electromagnetic response of the combined structure was clarified. It was found that the electric response of the combined structure is significantly affected by changing the thickness of the spacer. Moreover, we also examined the influence of periodicities on the LH transmission of the combined structure. It was demonstrated that the LH behavior is remarkably influenced by a_y while not by a_x. Finally, we propose a scheme of transmission to generalize the transmission properties as well as the LH behavior of the combined structure, based on the electric–magnetic correlation. It was shown that the LH behavior is predicted to be better, degraded or even destroyed by considering the overall electric–magnetic condition. Our results would be useful for a theoretical understanding and fabrication of combined metamaterials as well as an investigation of the feasibility of various applications.

Acknowledgments

The authors would like to thank Dr M H Cho at the Department of Mathematics and Statistics, University of North Carolina, at Charlotte, North Carolina, for his helpful discussions about the transfer matrix method. This work was supported by the National Foundation for Science and Technology Development (NAFOSTED 103.02.36.09) through the Institute of Materials Science, Vietnam Academy of Science and Technology.

References

[1] Veselago V G 1968 *Sov. Phys.—Usp.* **10** 509
[2] Smith D R, Padilla W J, Vier D C, Nermat-Nasser S C and Schultz S 2000 *Phys. Rev. Lett.* **84** 4184
[3] Pendry J B, Holden A J, Robbins D J and Stewart W J 1999 *IEEE Trans. Microw. Theory Tech.* **47** 2075
[4] Pendry J B, Holden A J, Stewart W J and Youngs I 1996 *Phys. Rev. Lett.* **76** 4773
[5] Zhou J, Koschny T, Zhang L, Tuttle G and Soukoulis C M 2006 *Appl. Phys. Lett.* **88** 221103
[6] Liu N, Guo H, Fu L, Kaiser S, Schweizer H and Giessen H 2007 *Adv. Mater.* **19** 3628
[7] Jylha L, Kolmakov I, Maslovski S and Tretyakov S 2007 *J. Appl. Phys.* **99** 043102
[8] Zhou J, Economou E N, Koschny T and Soukoulis C M 2006 *Opt. Lett.* **31** 3620
[9] Tung N T, Lam V D, Park J W, Cho M H, Lee Y P, Rhee J Y and Jang W H 2009 *J. Appl. Phys.* **106** 053109
[10] Drachev V P, Cai W, Chettiar U, Yuan H K, Sarychev A K, Kildishev A V, Klimeck G and Shalaev V M 2006 *Laser Phys. Lett.* **3** 49
[11] Guven K, Caliskan M D and Ozbay E 2006 *Opt. Express* **14** 8685
[12] Valentine J, Zhang S, Zentgraf T, Ulin-Avila E, Genov D A, Bartal G and Zhang X 2008 *Nature* **55** 376
[13] Markos P and Soukoulis C M 2001 *Phys. Rev.* B **65** 033401
[14] Penciu R S, Kafesaki M, Gundogdu T F, Economou E N and Soukoulis C M 2006 *Photonics Nanostruct. Fundam. Appl.* **4** 12
[15] Kafesaki M, Koschny Th, Penciu R S, Gundogdu T F, Economou E N and Soukoulis C M 2005 *J. Opt. A: Pure Appl. Opt.* **7** S12
[16] Tung N T, Hoai T X, Lam V D, Thuy V T T and Lee Y P 2010 *Eur. Phys. J.* B **74** 47
[17] Lam V D, Kim J B, Lee Y P and Rhee J Y 2007 *Opt. Express* **15** 16651
[18] Koschny T, Kafesaki M, Economou E N and Soukoulis C M 2004 *Phys. Rev. Lett.* **93** 107402
[19] Alici K B and Ozbay E 2008 *Photonics Nanostruct. Fundam. Appl.* **6** 102
[20] Pendry J B 1994 *J. Mod. Opt.* **41** 209
[21] www.cst.com
[22] Chen X, Grzegorczyk T M, Wu B I, Pacheco J and Kong J A 2004 *Phys. Rev.* E **70** 016608
[23] Lam V D, Kim J B, Tung N T, Lee S J, Lee Y P and Rhee J Y 2008 *Opt. Express* **16** 5934
[24] Tung N T, Lam V D, Cho M H, Park J W, Lee S J, Jang W H and Lee Y P 2009 *IEEE Trans. Magn.* **45** 4310

[25] Lam V D, Kim J B, Lee S J and Lee Y P 2008 *J. Appl. Phys.* **103** 033107
[26] Zhou J, Zhang L, Tuttle G, Koschny T and Soukoulis C M 2006 *Phys. Rev.* B **73** 041101
[27] Zhou J, Koschny T, Kafesaki M and Soukoulis C M 2008 *Photonics Nanostruct.: Fundam. Appl.* **6** 96
[28] Zhang S, Fan W J, Panoiu N C, Malloy K J, Osgood R M and Brueck S R J 2005 *Phys. Rev. Lett.* **95** 137404
[29] Boardman A D, King N and Velasco L 2005 *Electromagnetics* **25** 365
[30] McCall M W, Lakhtakia A and Weiglhofer W S 2002 *Eur. J. Phys.* **23** 353
[31] Depine R A and Lakhtakia A 2004 *Microw. Opt. Technol. Lett.* **41** 315
[32] Lam V D, Tung N T, Cho M H, Park J W, Jang W H and Lee Y P 2009 *J. Phys. D: Appl. Phys.* **42** 115404
[33] Lomakin V, Fainman Y, Urzhumov Y and Shvets G 2006 *Opt. Express* **14** 11164
[34] Cai W, Chettiar U K, Yuan H K, de Silva V C, Kildishev A V, Drachev V P and Shalaev V M 2007 *Opt. Express* **15** 3333
[35] Prodan E, Radloff C, Halas N J and Nordlander P 2003 *Science* **302** 419
[36] Lam V D, Tung N T, Cho M H, Park J W, Rhee J Y and Lee Y P 2009 *J. Appl. Phys.* **105** 113102
[37] Vu D L, Pham V T, Do T V, Nguyen T T, Thuy Vu T T, Le V H and Lee Y P 2010 *Adv. Nat. Sci.: Nanosci. Nanotechnol.* **1** 045016
[38] Lu Y, Jin X, Lee S, Rhee J Y, Jang W H and Lee Y P 2010 *Adv. Nat. Sci.: Nanosci. Nanotechnol.* **1** 045004
[39] Thuy Vu T T, Nguyen T T, Rhee J J, Vu D L and Lee Y P 2011 *Adv. Nat. Sci.: Nanosci. Nanotechnol.* **2** 015003